

Detection of non-volatile inorganic oxidizer-based explosives from wipe collections by infrared thermal desorption – direct analysis in real time mass spectrometry

Thomas P. Forbes*, Edward Sisco, and Matthew Staymates

National Institute of Standards and Technology, Materials Measurement Science Division, Gaithersburg, MD, USA.

ABSTRACT: Infrared thermal desorption (IRTD) was coupled with direct analysis in real time mass spectrometry (DART-MS) for the detection of both inorganic and organic explosives from wipe collected samples. This platform generated discrete and rapid heating rates that allowed volatile and semi-volatile organic explosives to thermally desorb at relatively lower temperatures, while still achieving elevated temperatures required to desorb non-volatile inorganic oxidizer-based explosives. IRTD-DART-MS demonstrated the thermal desorption and detection of refractory potassium chlorate and potassium perchlorate oxidizers, compounds difficult to desorb with traditional moderate-temperature resistance-based thermal desorbers. Nanogram to sub-nanogram sensitivities were established for analysis of a range of organic and inorganic oxidizer-based explosive compounds, with further enhancement limited by the thermal properties of the most common commercial wipe materials. Detailed investigations and high-speed visualization revealed conduction from the heated glass-mica base plate as the dominant process for heating of the wipe and analyte materials, resulting in thermal desorption through boiling, aerosolization, and vaporization of samples. The thermal desorption and ionization characteristics of the IRTD-DART technique resulted in optimal sensitivity for the formation of nitrate adducts with both organic and inorganic species. The IRTD-DART-MS coupling and IRTD in general offer promising explosive detection capabilities to the defense, security, and law enforcement arenas.

The need for trace explosives, narcotics, and other contraband detection for both security screening and in the field remains essential to the defense sector, homeland security, customs and border patrol, transportation security, law enforcement, and the forensic science community. This need, in concert with the ongoing threat posed by explosive-based terrorist attacks, continues to drive the technical advancement of detection instrumentation.¹ Nearly all available analytical techniques have been employed in some way for the detection, identification, or analysis of explosive compounds.²⁻⁶ However, portable benchtop or handheld instrumentation that is easy to operate and maintains attractive size, weight, and power (SWaP) parameters are more frequently deployed for screening or presumptive field detection applications. Most often, this includes techniques such as ion mobility spectrometry (IMS),⁷⁻¹⁴ Raman or Fourier transform infrared (FTIR) spectroscopies,¹⁵⁻¹⁸ or colorimetric sensors,¹⁹⁻²³ each of which provides rapid analyses at atmospheric pressure, providing sufficient sensitivity at reasonable cost. In general, many applications employ a dry wipe-based operating procedure for sample collection, in which a wipe, swab, or trap material is swiped across the target surface. Wipe collection enables larger surface areas, *e.g.*, vehicles, baggage, cargo, persons, or even post-blast debris, to be covered in a single sample analysis.

The thermal desorption of wipe-collected analytes is a widely deployed sample introduction step for trace explosives and narcotics detection for IMS,^{7, 10, 24-27} MS,²⁸⁻³¹ or fluorescence quenching.³² Often, these thermal desorbers utilize resistive heating of thermal mass(es) at a constant temperature. However, this causes difficulties with the efficient thermal desorption of compounds exhibiting vastly different chemical properties,

e.g., volatility, vapor pressure, melting and boiling points. These differences are readily apparent when considering various classes of explosives, most notably, differences between volatile peroxide-based (*e.g.*, TATP: triacetone triperoxide) or nitrate ester (*e.g.*, EGDN: ethylene glycol dinitrate) explosives and inorganic fuel-oxidizer mixtures (*e.g.*, icing sugar/potassium chlorate). In addition, common operating temperatures for thermal desorption of organic explosive and narcotic compounds are sorely inefficient for the thermal desorption of low vapor pressure refractory salts, most notably chlorate and perchlorate salts. Comparable difficulties arise with significantly raising the steady state temperature of thermal desorption – mainly, the thermal decomposition or degradation of labile species.

A few recent techniques and platforms have been developed to address hurdles with the thermal desorption of chlorate and perchlorate oxidizers while maintaining capabilities to analyze more volatile materials. One technique, implemented for thermal desorption with both atmospheric pressure chemical ionization mass spectrometry (APCI-MS)³³ and IMS,^{33, 34} incorporates a chemical conversion step prior to thermal desorption. This conversion is based on the acidic reagent-based conversion of these refractory salts to chloric and perchloric acids with easier to obtain thermal desorption temperatures. Use of both liquid and solid-state reagents have demonstrated significant increases in the signal of associated anions,³³ however, the incorporation of acidic reagents and an additional sample preparation step present hurdles in implementation for screening and fieldable applications. Other recent platforms have explored avenues for generating short discrete temperatures ramps to elevated temperatures to achieve thermal de-

sorption of inorganic salts.³⁵⁻³⁸ Recently, we reported on the development of an infrared thermal desorption (IRTD) platform for the wipe-based analyte desorption of *organic* explosive and illicit narcotic samples.³⁶ The IRTD technique enabled heating rates on the order of seconds, desorbing materials at their optimal temperatures. This preliminary work coupled IRTD with APCI-MS and focused on the development of IRTD as an energy efficient alternative (discrete 5 s infrared emission intervals) to the steady state continuously powered resistive heating oven type thermal desorbers for fieldable applications.³⁶ The AC corona discharge only maintained a 50 % duty cycle in the target ion mode and yielded large ion distributions, hindering target ion sensitivity. To alleviate these difficulties and enable the evolution of IRTD for the analysis of inorganic salts, we developed a next generation platform coupling IRTD with DART-MS through an enclosed junction.

In this Technical Note, we present the first demonstration of IRTD-DART-MS and its capabilities for the thermal desorption and detection of refractory chlorate and perchlorate oxidizers, which has traditionally been a substantial challenge at thermal desorption temperatures implemented for organic species detection. The near infrared emitter enabled discrete emission intervals, generating a rapid heating ramp that thermally desorbed more volatile organic explosives at low(er) temperatures, while still achieving elevated temperatures necessary to thermally desorb chlorate and perchlorate salts, during extended 10 s to 20 s emission intervals. Real-time temperature measurements of the thermal desorber unit were combined with extracted ion chromatograms, characterizing the heating processes to elevated temperatures and analyte detection. Nanogram to sub-nanogram sensitivities were demonstrated for both organic explosives and inorganic oxidizers by IRTD-DART-MS. Finally, the IRTD-DART sample introduction platform was coupled with a compact single quadrupole mass analyzer, demonstrating an avenue for rapid field deployable detection of low volatility inorganic oxidizers.

Experimental Methods

Materials. Single compound organic explosive standards were purchased at 1 mg/mL concentration from AccuStandard Inc. (New Haven, CT, USA)*, including, hexamethylene triperoxide diamine (HMTD), pentaerythritol tetranitrate (PETN), cyclotrimethylenetrinitramine (RDX), and 2,4,6-trinitrophenyl-methylnitramine (Tetryl). Stock concentrations were diluted in acetonitrile as required. Inorganic salts, including ammonium nitrate (AN), calcium ammonium nitrate (CAN), potassium chlorate (PC), and potassium perchlorate (PPC) were purchased from Sigma Aldrich (St. Louis, MO, USA) or EuroChem Agro (Mannheim, Germany) then dissolved and diluted in water to appropriate concentrations. Analytes were solution deposited directly onto sample collection wipes (polytetrafluoroethylene, PTFE-coated fiberglass weave: DSA Detection, LLC, Boston, MA, USA; Nomex swab: Smiths Detection, Hertfordshire, UK).

* Certain commercial products are identified in order to adequately specify the procedure; this does not imply endorsement or recommendation by NIST, nor does it imply that such products are necessarily the best available for the purpose.

Instrumentation. A twin tube near infrared emitter (Heraeus Noblelight America, LLC, Buford, GA, USA) was fixed within an aluminum thermal desorber enclosure (Figure 1(inset)). Both aluminum and glass-mica ceramic insulator (Mykroy/Mycalex) materials were employed for the bottom

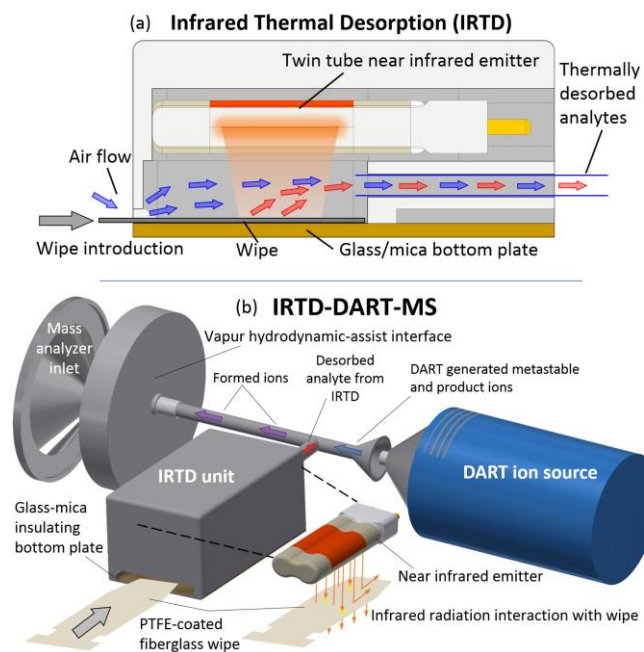


Figure 1. Schematic representation of the IRTD-DART-MS front-end platform. Components include: twin tube near infrared emitter housed within an aluminum enclosure with glass/mica bottom plate, a ceramic/glass/metal T-junction, DART ion source, and Vapor interface to time-of-flight mass analyzer. Inset: cross-sectional view of IRTD unit with wipe introduction and desorbed analyte flow.

plate – the location of wipe insertion and impinging infrared irradiation. The commercial AccuPower 120 Manual power supply (Heraeus Noblelight America, LLC) provided manipulation of infrared emission power level (percent maximum) and emission interval duration. The emitter's spectral distribution can be approximated as a black body emitter at around 2200 °C (filament temperature). Additional details of the infrared heater can be found in the literature.³⁶ The IRTD unit was connected to the mass spectrometer through a hybrid glass/ceramic/metal junction (6.35 mm OD, junction-to-IRTD: 4 cm, junction-to-Vapor: 7.5 cm, junction-to-flare: 4.5 cm) and Vapor hydrodynamic-assist interface, pulling at 4 L/min (Figure 1). This junction was heated by the DART gas stream and wrapped in insulation to maintain quasi-steady state temperatures, minimizing analyte condensation during transit. Ionization was achieved by the DART source (IonSense, Saugus, MA, USA) in an on-axis configuration, approximately 2 mm to 3 mm from the junction inlet. The DART source was operated with nitrogen at approximately 1.5 L/min, with gas stream maintained at 350 °C and a 100 V grid voltage. Preliminary work has demonstrated improved sensitivities for nitrogen DART gas relative to helium for the enclosed junction geometry. The IRTD-DART platform was operated with a JEOL JMS-T100LP AccuTOF (JEOL USA, Peabody, MA, USA) time-of-flight mass analyzer for most of this work. Detection was also demonstrated with a compact single quadrupole mass analyzer, the AQUITY QDa (Waters Corporation, Milford, MA, USA). Additional details of the

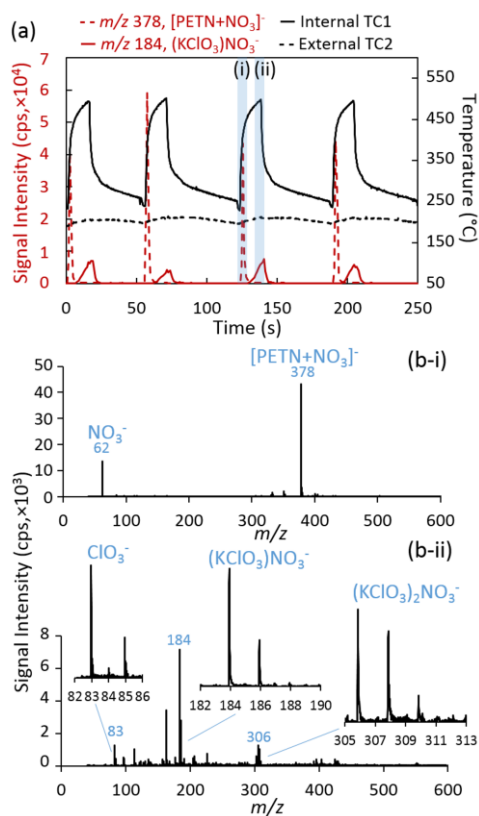


Figure 2. (a) Representative IRTD-DART-MS extracted ion chromatograms (XICs) of the PETN nitrate adduct (m/z 378) and PC nitrate adduct (m/z 184) for 15 s and 100 % power infrared emission intervals with associated thermocouple temperature measurements – 4 successive wipe-based sample replicates. (b) Corresponding mass spectra at time points representative of (b-i) PETN and (b-ii) PC desorption and detection.

AccuTOF and QDa mass spectrometer settings, as well as details of support instrumentation and measurements can be found in the supporting information, including temperature measurements, resistance-based thermal desorption, visualization, and sample quantification.

Results and Discussion

The IRTD-DART-MS platform, as displayed in Figure 1, was investigated for the thermal desorption of inorganic oxidizers as well as organic explosives. Continuous real-time temperature measurements of the bottom plate – the location of the inserted wipe and directed infrared emission – were taken both internally and externally. The internal thermocouple (TC1) resided within a small trench down the centerline of the bottom plate and recorded temperature measurements of the glass-mica plate at the focused area of the infrared emission (Figure S1). This thermocouple also experienced emitted radiation that was transmitted through the wipe material. The external thermocouple (TC2) measured the backside temperature of the bottom plate and therefore did not directly experience infrared irradiation. In an effort to maintain repeatability of desorber conditions at the initiation of each investigation, a number of infrared emission periods were conducted before experiments began. This led to the heating of the bottom plate and corresponding ceramic lines and junction components, resulting in a quasi-steady state operation (Figure S2).

Figure 2(a) displays temperature measurements and extracted ion chromatograms (XICs) from four successive replicate wipe-based samples. Each wipe contained 10 ng PETN and

500 ng PC, and was exposed to a 15 s emission interval at 100 % power. Most investigations of the chlorate and perchlorate salts demonstrated here also included an organic species to aid in correlating temperature and ion chromatogram data. At the initiation of each emission interval, the internal thermocouple (TC1) experienced a rapid increase in temperature. Beyond the 5 s intervals used in our previous work,³⁶ as the temperatures reached elevated levels, PC desorption and detection was observed. Figure 2(b) displays representative mass spectra from the early desorption of PETN (Figure 2(b-i)) and later desorption of PC (Figure 2(b-ii)). PETN predominately formed a nitrate adduct, m/z 378 $[\text{PETN}+\text{NO}_3]^-$, as commonly observed in prior DART-MS work.³⁹⁻⁴¹ The rapid heating ramp enabled organic species to desorb at lower temperatures, avoiding thermal degradation at higher temperatures. No excess PETN fragmentation or degradation products were observed beyond that expected with, and attributed to, the base in-source collision induced dissociation parameters (more details below). Similarly, potassium chlorate also predominantly formed a nitrate adduct, m/z 184 $(\text{KClO}_3)\text{NO}_3^-$, as well as additional peaks for the chlorate anion, m/z 83 ClO_3^- , and a dimer nitrate adduct, m/z 306 $(\text{KClO}_3)_2\text{NO}_3^-$, along with appropriate isotopic distributions (Figure 2(b-ii)). In-source collision induced dissociation (CID) was employed to directly control the extent of adduct and cluster formation and fragmentation (Figure S3). This method has been implemented with solid-liquid extraction-,^{42, 43} laser-,⁴⁴ and plasma-based^{35, 45} techniques to optimize for the molecular anion of inorganic oxidizers or elemental cations from other inorganic explosive device signatures. Here, a mid-range in-source CID (*i.e.*, 20 V) yielded the optimal performance for both the PC- and PETN-nitrate adducts (additional details in supporting information, Figure S3). The preservation of the intact salt species (KClO_3) allows for more robust detection and identification of the original species in certain cases. Alternative techniques targeting the anions (*e.g.*, ClO_3^-), typically lose chemical information of the original oxidizer species. It is important to note that the preservation of the intact salt species will be a direct function of the ionic bond strength. For example, species such as potassium chlorate with high(er) enthalpies of formation (-397.7 kJ/mol) retained their original cation-anion pairing as demonstrated here.⁴⁴ However, species with lower enthalpies of formation, such as ammonium perchlorate (NH_4ClO_4 , -295.8 kJ/mol) readily fragmented, predominately exhibiting the bare anion (Figure S4).

We further investigated the desorption and detection of PC as a function of infrared emitter parameters. For the thermal desorption of these refractory salts, maximum temperatures were required, therefore, 100 % emission power was considered optimal. Figure 3(a) displays the real-time temperature measurements and corresponding extracted ion chromatograms for representative examples at 10 s, 15 s, and 20 s emission intervals. As the emission interval increased, the extracted ion chromatogram for PC followed a self-similar profile, with signal increasing further up the desorption profile with each extension in the interval. The rapid thermal desorption of PETN, within a few seconds of initiating the infrared emission, led to minimal differences in the extracted ion chromatogram. This was not surprising given the reproducible nature of the temperature profiles (Figure 3(a)). Figure 3(b) displays average peak area of replicate 250 ng PC and 10 ng PETN samples as a function of increasing emission duration. An 8 s emission interval at 100 % was the minimum time required for detection of 250 ng of PC. Further increasing the emission time steadily

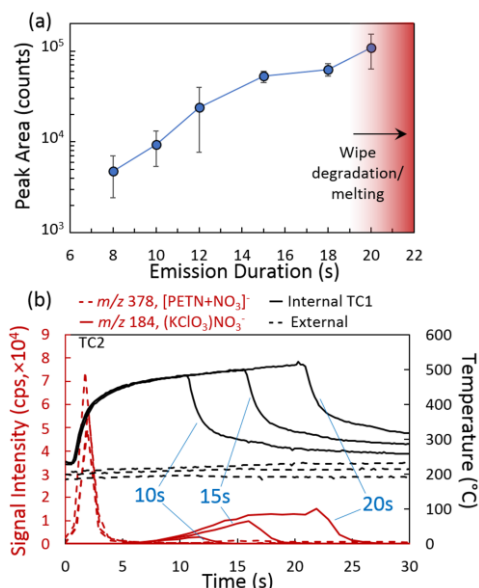


Figure 3. (a) Representative XICs of the PETN nitrate adduct and PC nitrate adduct with associated thermocouple temperature measurements for 10 s, 15 s, and 20 s IRTD emission intervals. (b) IRTD-DART-MS peak area of the PC nitrate adduct (m/z 184, $(\text{KClO}_3)\text{NO}_3^-$) from 250 ng samples as a function of infrared emission interval duration. Data points and uncertainty represent the average peak area and standard deviation from five replicate measurements.

increased the average peak areas up to 20 s, at which point melting and decomposition of the wipe material began, leading to irreproducibility and large relative standard deviation. However, below the 20 s threshold (e.g., 15 s), the wipes were reusable without observed detrimental effects when allowed to cool to room temperature between emission intervals (Figures S5). Extraction and quantification of remaining material demonstrated incomplete desorption of PC within the emission interval limitations imposed by wipe melting (Figure S5, additional details in supporting information). Other commercially available wipe materials, e.g., Nomex, muslin, or paper, absorbed significant amounts of near infrared radiation and more readily melted or charred. However, other groups have introduced alternative wipe materials and coatings, e.g., phenyl silanes, aimed at higher temperature thermal desorption that may provide enhancement here.^{46, 47}

The IRTD-DART-MS platform's ability to thermally desorb and detect chlorate and perchlorate salts from commercially available wipe materials demonstrates a powerful capability for explosive detection instrumentation employing thermal desorption for sample vaporization and introduction. We conducted a preliminary evaluation of both inorganic and organic species sensitivities (representative mass spectra can be found in the supporting information, Figure S6). Table 1 displays the explosives considered, compound classification, selected ion observed, m/z value, deposited mass (directly onto wipe), and signal-to-noise ratio (S/N). S/N ratios were derived directly from the selected extracted ion chromatogram signal and corresponding $3\times$ the standard deviation of the background noise. The IRTD-DART-MS platform demonstrated notable sub-nanogram sensitivities for the nitrate-based explosives considered, down into the 10's of picograms for RDX. The 5 ng to 10 ng sensitivities for PC and PPC salts demonstrated a significant enhancement over traditional thermal desorption platforms.

Table 1. Trace level detection for inorganic oxidizer-based and organic explosive compounds. Selected ions and corresponding signal-to-noise ratios (S/N) from deposited masses.^a

Compound	Ion Observed	m/z	Mass (ng)	S/N ^b
Inorganic Oxidizers				
PC	$(\text{KClO}_3)\text{NO}_3^-$	184	10	7 ± 3
PPC	$(\text{KClO}_4)\text{NO}_3^-$	200	5	5 ± 2
AN	$(\text{HNO}_3)\text{NO}_3^-$	125	10	8 ± 3
CAN	$(\text{HNO}_3)\text{NO}_3^-$	125	10	4 ± 2
Organic Explosives				
RDX	$[\text{M}+\text{NO}_3]^-$	284	0.05	6 ± 2
Tetryl	$[\text{M}-\text{NO}_2]^-$	241	0.2	5 ± 1
PETN	$[\text{M}+\text{NO}_3]^-$	378	0.1	9 ± 3
HMTD	$[\text{M}+\text{H}]^+$	209	20	9 ± 3

^a IRTD-DART-MS emission intervals of 15 s at 100 % were used.

^b S/N ratios and uncertainty represent the average and standard deviation from five replicate measurements.

The performance of the IRTD-DART-MS configuration was briefly compared with that of a TD-DART-MS configuration using a commercial resistance-based constant temperature thermal desorber.³⁰ Thermal desorber temperatures of both 240 °C, typical for organic species thermal desorption, and an elevated 300 °C, were used. Direct wipe temperature measurements for these conditions demonstrated that steady state temperatures matching the setpoint were reached within approximately 10 s (Figure S7). A 200 pg sample of PETN demonstrated comparable peak area between the IRTD and 240 °C TD analyses. At 300 °C, the TD-DART-MS PETN signal was reduced by approximately 3-fold. This demonstrates the unique value in using a rapid heating ramp instead of a constant elevated temperature. Similarly, for a 10 ng sample of AN, which exhibits a reasonable vapor pressure, classical TD resulted in 2.4-fold and 3.4-fold reductions in peak area relative to the 15 s / 100 % IRTD analysis. Finally, neither PC nor PPC were detected by TD-DART-MS for either 240 °C or 300 °C setpoint temperatures at loadings up to 250 ng (25 \times and 50 \times trace levels demonstrated in Table 1). Yet, the IRTD-DART-MS platform enabled the desorption and detection of nanogram levels of these inorganic oxidizer species.

Following the preliminary evaluation and performance measurements presented above, we next investigated the sample heating phenomena experienced in the IRTD. We noted strong absorption in the near infrared emission range of the lamp.³⁶ In combination with the negligible near infrared absorption of the PTFE-coated fiberglass weave wipe, the heat transfer path by direct infrared absorption of either the wipe or analyte was minimal. Here, we present a series of experiments supporting the hypothesis that the infrared emission predominantly transmitted through the sample wipe, some fraction was absorbed by the bottom plate, increasing its temperature, which finally conducted to the wipe material residing in loose contact on its surface (Figure 1(inset) and S1). This process was reinforced by the measured temperature profiles of the glass-mica bottom plate just beneath the wipe substrate (TC1) and on the external side (TC2). The combination of real-time temperature measurements of the bottom plate, extended infrared emission intervals, and direct visualization allowed us to develop a more comprehensive understanding of the heat transfer routes for analyte thermal desorption.

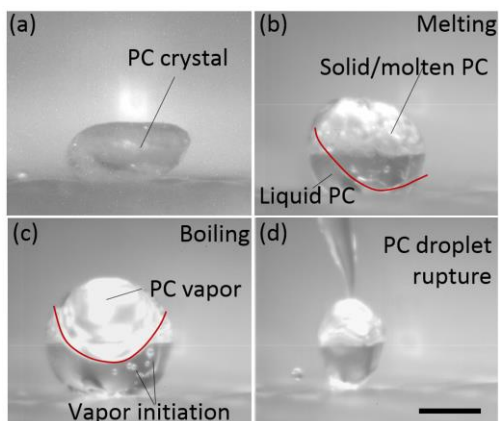


Figure 4. High speed visualization of IRTD heating of single PC crystal. Heating and melting initiates from the wipe surface, leading to boiling, atomization, and vaporization. Visualization was acquired at 9000 frames/s for (640 × 480) pixel images. Scale bar represents approximately 250 μm.

The heating of the wipe substrate and analyte by conduction from the glass-mica bottom plate was first investigated with high-speed visualization of the process. Figure 4 displays select images from a series of high-speed videos visualizing the heating of a single PC crystal placed onto the wipe surface and inserted into the IRTD unit. High-speed visualization identified an initial melting of the crystal (Video S1), during which the portion in contact with the wipe material appeared to liquify first. This substantiates the theory that heat transfer to the analytes of interest was dominated by conduction from a heated base plate over direct irradiation from above. The melting phenomena was followed by boiling and vapor generation within the liquid/molten PC drop (Video S1), initiating at the wipe surface. This vapor accumulated at the apex until the drop ruptured, ejecting a large portion of the molten PC. This atomization of molten droplets was observed from both residue (solution deposited, Videos S2) and crystal deposits (Videos S3 and S4).

In addition to the visualization data, an alternative aluminum bottom plate was considered. The geometry, wipe location, and thermocouple trench mirrored those in the glass-mica bottom plate (Figure S1). The temperature measurements from the aluminum plate under successive 15 s / 100 % power emission intervals failed to reach the temperatures achieved by the glass-mica plate (Figure S8). Even with extended emission times, *e.g.*, 30 s, aluminum temperatures only reached approximately 350 °C, no wipe melting or degradation was observed. As discussed above, wipe melting began for 20 s emission intervals with the glass-mica bottom plate. No PC signal was observed during any aluminum base plate experiments. The reduction in overall achieved temperatures and corresponding lack of any PC detection with an alternative base plate eliminated direct absorption of infrared irradiation as a major source of wipe and analyte heating. This convincing result further verified that a sufficient fraction of the infrared energy was absorbed by the glass-mica material, and subsequently conducted to the wipe substrate and analyte for thermal desorption. The glass-mica material provided a serendipitous combination of infrared absorption and heat retention without itself melting or decomposing. Optimization of this material (*e.g.*, alternative ceramic-based insulating materials), absorption properties (*e.g.*, targeted absorption in the near infrared range), and geometry (*e.g.*, thickness, contact with wipe, prox-

imity to emitter, etc.), should be the focus of future work to enhance thermal desorption and presumably sensitivity.

Finally, the IRTD-DART platform was coupled with a compact single quadrupole mass analyzer (AQUITY QDa) to demonstrate an avenue toward field portability. Both low volatility inorganic oxidizers, potassium chlorate and potassium perchlorate, were detected and exhibited a similar temporal response to that demonstrated for the time-of-flight mass analyzer (Figure S9). Specifically, the organic PETN explosive was thermally desorbed and detected shortly after the initiation of infrared radiation, while the chlorate and perchlorate salts desorbed near the end of the 15 s emission. A full parametric optimization of the single quadrupole coupling was not considered here and beyond the scope of this work. The quadrupole mass analyzer exhibited a reduction in sensitivity, therefore single ion recording (SIR) was employed. The IRTD-DART-QDa system demonstrated the detection of PC and PPC at 100 ng and 500 ng with S/N ratios of 34 and 50, respectively, providing an avenue for the *in situ* detection of non-volatile inorganic oxidizer-based explosives.

Conclusions

The coupling of infrared thermal desorption (IRTD) with DART-MS provided a powerful platform for the detection of both inorganic oxidizer and organic explosive species from wipe-based samples. The thermal desorption of target analytes from wipe-based collections remains standard operating procedure for a wide range of security, screening, forensic science, and other field deployable applications. The IRTD-DART-MS platform enabled the thermal desorption and detection of refractory chlorate and perchlorate salts typically used in fuel-oxidizer explosives, a capability difficult for traditional moderate temperature techniques targeting organic species. The investigation presented here not only demonstrated single to tens of nanograms sensitivities for a number of inorganic oxidizers, but also established sub-nanogram sensitivities for common nitrate-based organic explosives. The rapid heating rate aided in the thermal desorption of chemical species with widely varying chemical properties, each at its respective optimal temperature. Future work might enable further enhancements to this process through optimization of the material properties and geometry. In addition, alternative wipe materials with similar absorption spectra that could withstand higher temperatures would aid to improve the extent of PC and PPC desorption, further enhancing sensitivities. The IRTD-DART-MS not only demonstrated powerful capabilities for the detection of inorganic and organic explosives, but also introduces numerous opportunities for the coupling of IRTD-DART with portable mass analyzers or the coupling of IRTD with alternative ion sources and detection instrumentation, such as IMS.

ASSOCIATED CONTENT

Supporting Information

Additional experimental details, high speed visualization videos, figures, and MS spectra as noted in the text can be found in the online supporting information.

AUTHOR INFORMATION

Corresponding Author

* E-mail: thomas.forbes@nist.gov.

Notes

‡ Official contribution of the National Institute of Standards and Technology; not subject to copyright in the United States.

ACKNOWLEDGMENT

The U.S. Department of Homeland Security's Science and Technology Directorate sponsored a portion of the production of this material under Interagency Agreement IAA HSHQPM-15-T-00050 with the National Institute of Standards and Technology.

REFERENCES

- (1) National Consortium for the Study of Terrorism and Responses to Terrorism (START). <https://www.start.umd.edu/gtd>.
- (2) Caygill, J. S.; Davis, F.; Higson, S. P. J., *Talanta*, **2012**, *88*, 14-29.
- (3) Moore, D. S., *Rev. Sci. Instrum.*, **2004**, *75*, 2499-2512.
- (4) Yinon, J., *Trends Anal. Chem.*, **2002**, *21*, 292-301.
- (5) Yinon, J., *Counterterrorist Detection Techniques of Explosives*. Elsevier, B.V.: Amsterdam, 2007.
- (6) Forbes, T. P.; Sisco, E., *Analyst*, **2018**, DOI: 10.1039/C7AN02066J.
- (7) Ewing, R. G.; Atkinson, D. A.; Eiceman, G. A.; Ewing, G. J., *Talanta*, **2001**, *54*, 515-529.
- (8) Kolakowski, B. M.; Mester, Z., *Analyst*, **2007**, *132*, 842-864.
- (9) Oxley, J. C.; Smith, J. L.; Kirschenbaum, L. J.; Maringanti, S.; Vadlamannati, S., *J. Forensic Sci.*, **2008**, *53*, 690-693.
- (10) Najarro, M.; Davila Morris, M. E.; Staymates, M. E.; Fletcher, R.; Gillen, G., *Analyst*, **2012**, *137*, 2614-2622.
- (11) Tabrizchi, M.; Ilbeigi, V., *J. Hazard. Mater.*, **2010**, *176*, 692-696.
- (12) Ehler, S.; Walte, A.; Zimmermann, R., *Anal. Chem.*, **2013**, *85*, 11047-11053.
- (13) Liang, X.; Zhou, Q.; Wang, W.; Wang, X.; Chen, W.; Chen, C.; Li, Y.; Hou, K.; Li, J.; Li, H., *Anal. Chem.*, **2013**, *85*, 4849-4852.
- (14) Verkouteren, J. R.; Lawrence, J.; Klouda, G. A.; Najarro, M.; Grandner, J.; Verkouteren, R. M.; York, S. J., *Analyst*, **2014**, *139*, 5488-5498.
- (15) Gaft, M.; Nagli, L., *Opt. Mater.*, **2008**, *30*, 1739-1746.
- (16) Moore, D. S.; Scharff, R. J., *Anal. Bioanal. Chem.*, **2009**, *393*, 1571-1578.
- (17) Huang, F.; Schulkin, B.; Altan, H.; Federici, J. F.; Gary, D.; Barat, R.; Zimdars, D.; Chen, M.; Tanner, D. B., *Appl. Phys. Lett.*, **2004**, *85*, 5535-5537.
- (18) Mou, Y.; Rabalais, J. W., *J. Forensic Sci.*, **2009**, *54*, 846-850.
- (19) Lin, H.; Suslick, K. S., *J. Am. Chem. Soc.*, **2010**, *132*, 15519-15521.
- (20) Peng, Y.; Zhang, A.-J.; Dong, M.; Wang, Y.-W., *Chem. Commun.*, **2011**, *47*, 4505-4507.
- (21) Peters, K. L.; Corbin, I.; Kaufman, L. M.; Zreibe, K.; Blanes, L.; McCord, B. R., *Anal. Methods*, **2015**, *7*, 63-70.
- (22) SEEKERe, DetectaChem. <https://www.detectachem.com/>, Oct. 31, 2017.
- (23) Krauss, S. T.; Holt, V. C.; Landers, J. P., *Sens. Actuators B Chem.*, **2017**, *246*, 740-747.
- (24) IONSCAN 500DT, Smiths Detection. <https://www.smithsdetection.com/products/ionscan-500dt-2/>, April 13, 2018.
- (25) B220 Desktop Trace Detector, L3 Technologies, Inc. <http://www.sds.i-3com.com/etd/B220-desktop-ETD.htm>, April 13, 2018.
- (26) Eiceman, G. A.; Stone, J. A., *Anal. Chem.*, **2004**, *76*, 390 A-397 A.
- (27) Forbes, T. P.; Najarro, M., *Analyst*, **2016**, *141*, 4438-4446.
- (28) MX908, 908 Devices. <https://908devices.com/products/mx908/>, April 16, 2018.
- (29) Tracer 1000 MS-ETD, 1st Detect. <http://www.1stdetect.com/>, Oct. 31, 2017.
- (30) Sisco, E.; Forbes, T. P.; Staymates, M. E.; Gillen, G., *Anal. Methods*, **2016**, *8*, 6494-6499.
- (31) Popov, I. A.; Chen, H.; Kharybin, O. N.; Nikolaev, E. N.; Cooks, R. G., *Chem. Commun.*, **2005**, 1953-1955.
- (32) Fido X3, FLIR. <http://www.flir.com/home/>, Oct. 31, 2017.
- (33) Kelley, J. A.; Ostrinskaya, A.; Geurtsen, G.; Kunz, R. R., *Rapid Commun. Mass Spectrom.*, **2016**, *30*, 191-198.
- (34) Peng, L.; Hua, L.; Wang, W.; Zhou, Q.; Li, H., *Sci. Rep.*, **2014**, *4*, 6631.
- (35) Forbes, T. P.; Sisco, E.; Staymates, M.; Gillen, G., *Anal. Methods*, **2017**, *9*, 4988-4996.
- (36) Forbes, T. P.; Staymates, M.; Sisco, E., *Analyst*, **2017**, *142*, 3002-3010.
- (37) Krechmer, J.; Tice, J.; Crawford, E.; Musselman, B., *Rapid Commun. Mass Spectrom.*, **2011**, *25*, 2384-2388.
- (38) Vilkov, A. N.; Widjaja, J. A.; Syage, J. A. Temperature influenced chemical vaporization and detection of compounds having low volatility. US9689857B1, 2017.
- (39) Bridoux, M. C.; Schwarzenberg, A.; Schramm, S.; Cole, R. B., *Anal. Bioanal. Chem.*, **2016**, *408*, 5677-5687.
- (40) Sisco, E.; Forbes, T. P., *Analyst*, **2015**, *140*, 2785-2796.
- (41) Forbes, T. P.; Sisco, E., *Anal. Methods*, **2015**, *7*, 3632-3636.
- (42) Forbes, T. P.; Sisco, E., *Anal. Chem.*, **2014**, *86*, 7788-7797.
- (43) Evans-Nguyen, K. M.; Quinto, A.; Hargraves, T.; Brown, H.; Speer, J.; Glatter, D., *Anal. Chem.*, **2013**, *85*, 11826-11834.
- (44) Forbes, T. P.; Sisco, E., *Anal. Chim. Acta*, **2015**, *892*, 1-9.
- (45) Evans-Nguyen, K. M.; Gerling, J.; Brown, H.; Miranda, M.; Windom, A.; Speer, J., *Analyst*, **2016**, *141*, 3811-3820.
- (46) Addleman, R. S.; Atkinson, D. A.; Bays, J. T.; Chouyyok, W.; Cinson, A. D.; Ewing, R. G.; Gerasimenko, A. A. Enhanced surface sampler and process for collection and release of analytes. US8943910 B2, 2015.
- (47) Addleman, R. S.; Li, X. S.; Chouyyok, W.; Atkinson, D. A. Collection, release, and detection of analytes with polymer composite sampling materials. US20160313218 A1, 2015.